JNeurosci
THE JOURNAL OF NEUROSCIENCE

Research Articles: Behavioral/Cognitive

Neurons in the monkey's subthalamic nucleus differentially encode motivation and effort

https://doi.org/10.1523/JNEUROSCI.0281-21.2021

Cite as: J. Neurosci 2022; 10.1523/JNEUROSCI.0281-21.2021

Received: 4 February 2021
Revised: 12 July 2021
Accepted: 17 August 2021

TITLE

Neurons in the monkey's subthalamic nucleus differentially encode motivation and effort

ABBREVIATED TITLE

Motivation and effort in monkey's STN

AUTHORS

Simon Nougaret[1], Christelle Baunez[1] and Sabrina Ravel[1]

AFFILIATIONS

[1] Institut de Neurosciences de la Timone, UMR7289, Centre National de la Recherche Scientifique and Aix-Marseille Université, France.

SUBMITTING AND CORRESPONDING AUTHOR

Simon Nougaret

Institut de Neurosciences de la Timone, UMR 7289, Aix-Marseille Université and CNRS, Campus Santé Timone, 27 bd Jean Moulin, 13385 Marseille, France.

simon.nougaret@univ-amu.fr

CONFLICT OF INTEREST

The authors declare no competing financial interests.

ACKNOWLEDGMENTS

This work was supported by Centre National de la Recherche Scientifique, the Aix-Marseille Université, the Fondation de France (Parkinson's Disease Program Grant 2008 005902 to SR) and the Agence Nationale de la Recherche (ANR STNmotiv: ANR-09-MNPS-028-01 to CB).

NUMBER OF PAGES: 31

NUMBER OF FIGURES: 6

NUMBER OF WORDS FOR ABSTRACT: 187

NUMBER OF WORDS FOR INTRODUCTION: 720

NUMBER OF WORDS FOR DISCUSSION: 2232

ABSTRACT

The understanding of the electrophysiological properties of the subthalamic nucleus (STN) neurons is crucial since it represents the main target of deep brain stimulation for the treatment of Parkinson's Disease and obsessive compulsive disorders. The study of its non-motor properties could shed light on the cognitive and motivational alterations possibly encountered after stimulation. In this study, we recorded the activity of STN neurons in two male behaving monkeys (*Macaca mulatta*) while they performed a visuomotor motivational task in which visual cues indicated which amount of force was required to obtain which amount of reward. Our results evidenced force- and reward-modulated neurons. After the occurrence of the visual stimuli, the force-modulated neurons mainly fired when a high effort was required. Differently, the activity of the population of reward-modulated neurons encoded the motivational value of the stimuli. This population consisted of neurons increasing or decreasing their activity according to the motivational ranking of the task conditions. Both populations could play complementary roles, one in the implementation of the difficulty of the action and the other in enhancing or slowing its execution based on the subjective value of each conditions.

SIGNIFICANT STATEMENT

An increasing number of studies confers a role to the subthalamic nucleus (STN) in motivational and reward-related processes. However, the electrophysiological bases of such properties at the neuronal level remains unclear. The present study investigated the modulation of STN neuronal activity in monkeys performing a motivational task in which the force to produce and the reward obtained were manipulated. We found two main populations of neurons, one modulated by the effort required and the other integrating the motivational subjective value of the stimuli. This last population could help at improving decision-making to act or not, depending on the subjective value set by the motivational context. This highlights the pivotal role of STN in valuation of cost/benefit for decision-making processes.

KEYWORDS

Subthalamic nucleus – Monkey – Reward – Effort – Motivation – Electrophysiology

INTRODUCTION

Clinical and experimental data have shown that the basal ganglia (BG) are involved in goal-directed behaviors and play a role in several processes including selection and execution of actions, but also reward-related learning and integration of reward value. The subthalamic nucleus (STN) is considered as one of the two main input structures of the BG with the striatum, since it receives direct inputs from the cortex via the hyper-direct pathway (Nambu et al. 2002; Haynes and Haber 2013). The involvement of the STN in motivational processes is supported first anatomically by the presence of direct projections from the ventromedial prefrontal cortex, the orbitofrontal cortex and the anterior cingulate cortex (Takada et al. 2001, Nambu et al. 2002, Haynes and Haber, 2013, Nougaret et al. 2013), known for their pivotal role in the integration of reward information. Second, STN lesion and deep brain stimulation (DBS) studies in rodents have shown its involvement in impulsivity and perseverative behaviors towards sweet food reward (Baunez and Robbins 1997, Baunez et al. 2002), opposite motivation for natural reward and drug of abuse (Baunez et al. 2005; Rouaud et al 2010) and that it could affect the amount of salience allocated to stimuli conveying reward-related information (Baunez et al 2002; Uslaner et al. 2008). Accordingly, numbers of clinical studies using DBS to treat motor symptoms of Parkinson's disease (PD) reported cognitive and motivational side effects such as impulsive choices and alteration of decision-making (Frank et al. 2007, Cavanagh et al. 2011, Coulthard et al. 2012). Third, electrophysiological recordings acquired in PD patients while performing cognitive tasks revealed strong relationships between the oscillatory activity of the local field potential (LFPs) of the STN and the mecanisms of response inhibition and regulation of decision processes (Cavanagh et al. 2011, Brittain et al. 2012, Zavala et al. 2014). Studying the STN LFP oscillations also revealed that the subjective cost of an action, the subjective value of a reward (Zenon et al. 2016) and the specific motor effort to assign to a motor response are represented at STN level (Tan et al. 2015) and that this structure is involved in monetary reward processing (Fumagelli et al. 2015) and economic decisions (Rosa et al. 2013). Moreover, electrophysiological data from behaving rodents and non-human primates indicate that STN neurons are modulated by cues predicting reward and reward occurrence (Matsumura et al., 1992 ; Darbaky et al., 2005; Teagarden and Rebec, 2007; Lardeux et al., 2009, 2013; Espinosa-Parrilla et al 2013, 2015 ; Breysse et al 2015), that they could link reward information to the motor output (Espinosa-Parrilla et al., 2013) and differentiate reward types and relative values of reward (Lardeux et al., 2009 ; 2013 ; Breysse et al 2015 ;

Espinosa-Parrilla et al 2015). The STN activity correlates with the discharge balance and produce a matching change of the BG downstream structure (Deffains et al. 2016). By acting on the output structures of the BG, STN could suppress undesired mouvements by stimulating their inhibitory influence (Isoda and Hikosaka, 2008 ; Mink, 1996), but conversely, it could thus also enhance some actions by alleviating this influence, impairing decision-making (Frank 2006). Taken together, these studies suggest a critical role of the STN in decision-making and motivated behaviors and a strategic position in the cortico-BG-cortical loops involving the prefrontal cortices.

It remains unknown however how these functions are exerted at single-cell level by STN neurons and particularly how two major components of a motivated behavior, the effort it requires and the benefit it brings, are integrated. To this aim, the activities of STN neurons were recorded while monkeys had to exert one of two possible levels of force on a lever to gain one reward of two possible magnitudes. Visual stimuli, displayed simultaneously, were used to indicate to the animals the level of force required and reward magnitude on board. They set a motivational value for each condition and triggered the movement. Activities were analysed after stimuli occurrence, to examine whether these two variables were encoded by the same or by different populations of neurons. Our data suggest that a population of STN neurons encode mainly the effort to be produced when a high effort is required, whereas another population of STN neurons not only encode the expected reward, but the subjective motivational value of the action requiring integration of reward and force values.

MATERIAL AND METHODS

Animal and Apparatus

We trained two male rhesus monkeys (Macaca mulatta), weighing 8 and 7 kg at the beginning of the experiments (Monkeys M and Y, respectively), to apply and maintain a pressing force on a lever in response to visual cues to receive a liquid reward. All experimental procedures were in compliance with the National Institutes of Health's Guide for the Care and Use of Laboratory Animals, the French laws on animal experimentation, and the European Directive on the protection of animals used for scientific purposes.

Behavioral Procedures

The monkeys were seated in a Plexiglas primate chair and in front of a panel supporting a 17-in. screen on which visual cues could be presented. It was positioned 18 cm from the monkey.

A lever outfitted with strain gauges in the lower part of the panel was positioned at waist level. At the front panel of the primate chair, a sliding door was opened to allow the animal to position its hand on the lever. The liquid reward (apple sauce diluted with water) was delivered through a distributor equipped with a peristaltic pump installed outside the recording room and released via a metal spout positioned directly in front of the monkey's mouth. Figure 1A illustrates the trial schedule. At the beginning of a trial, the monkeys had to develop a basal pressing force on the lever during a 1-sec preparatory period. This force was determined as between 0% and 20% of the maximal force, experimentally defined at 900 g based on the capabilities of the animals. After this preparatory period, two visual cues, a green one and a red one, each being either a filled circle or a filled square, were displayed vertically in the center of the screen. Their shapes indicated, for the green stimulus, the level of force the animals had to produce on the lever, and for the red stimulus the size of the upcoming reward. A green circle indicated that the animals had to produce a force between 20% and 55% of the maximal force (180–495 g; low force: f) and a green square, a force between 55% and 90% of the maximal force (495–810 g; high force: F). Similarly, a red circle indicated to the animals that they could receive a small amount of reward (0.3 mL; small reward: r), whereas a red square indicated that a large amount of reward could be delivered (1.2 mL; large reward: R). Consequently, there were four possible combinations of cues (fR, FR, fr, and Fr) that set the four different conditions of the task. In response to a pair of stimuli, monkeys had to increase their pressing force on the lever to reach the required force in a period shorter than 1 sec and hold this force for 1 sec (holding time) to get the reward. According to the shape of the red stimulus, monkeys were rewarded with a small or large reward for each correct trial. The pair of stimuli was extinguished as soon as the reward was delivered. A vertical rectangle representing the range of the required force, located below the pair of stimuli, helped the monkeys to reach the required force. Indeed, a white cursor diplayed in the rectangle indicated the force developed on the lever in real time when they were in the required force range. To keep cues constant across trial conditions, the animals saw the same rectangle for both the low and high force ranges. Once the reward was delivered, the monkeys returned to a basal pressing force in preparation for the next trial. The next trial did not begin until the total duration of the current trial had elapsed, i. e. 4.5 sec regardless of the animal behavior. Monkeys could fail to perform a trial in three different cases. First, they did not reach the required force within the 1-sec force development period. These trials were considered as "omission errors". Second, they did not hold the required force for at least 1 sec (holding time). These trials were considered as "holding errors". Last,

they developed a force which was greater than the upper limit of the required force (495 and 810 g for the low and high forces, respectively). These trials were considered as "threshold errors". After an error, the same condition was presented again to the monkeys until they performed the trial correctly in order to prevent the monkey avoiding the trials of a particular condition. Moreover, trials in which the monkeys began to increase their pressing force within 100 msec after the occurrence of the cues were considered as anticipations and were excluded from the database. Both monkeys were extensively trained (4–6 months) until they achieved a performance of 80% of correct trials. In each recording session, the four different conditions were displayed pseudorandomly from trial to trial. The same condition was not displayed more than three times sequentially if trials were performed correctly.

Surgery

The surgery protocol was the same than previously described in Nougaret and Ravel (2015, 2018). Under anesthesia (first intramuscular injection of ketamine (10 mg/ kg) and xylazine (0.5 mg/ kg), followed by deep anesthesia induced by isoflurane), two monkeys were implanted over the left hemisphere with a polyether-ether-ketone (PEEK) recording chamber (19-mm inner diameter). These recording chambers were positioned with a 20° angle laterally in the coronal plane. For Monkey M, the targeted stereotaxic coordinates, relative to the ear bars, were +18 mm on the antero-posterior axis and +16 mm in laterality. For Monkey Y, they were + 14 mm in the antero-posterior axis and + 16 mm in laterality. These landmarks were based on the atlas of Saleem and Logothetis (2007). Moreover, a device for head restraint for the future neuronal recordings composed of two titanium cylinders embedded in orthopedic cement (Palacos with gentamycin) was fixed to the skull with titanium orthopedic bone screws. Antiobiotics (Marbocyl, 2 mg/ kg) and analgesics (Tolfedine, 4 mg/ kg) were administrated to the monkeys on the day of the surgery and for the 4 following days. The antibiotics (Marbocyl, 2 mg/mL) were also used to fill the recording chamber before sealing it with a removable cap.

Electrophysiological Recordings

The extracellular activity of single neurons was recorded with microelectrodes while the monkeys performed the task with head immobilization. These microelectrodes were custom-made with glass-insulated tungsten following the technique of Merrill and Ainsworth (1972). To reach the BG structures, the microelectrode was inserted inside a stainless-steel guide tube (diameter = 0.6 mm) lowered below the surface of the dura, and was advanced using a manual

hydraulic microdrive (M096; Narishige). The microelectrode was connected to a preamplifier situated close to the microdrive. The electric signal was then amplified 5,000 times and filtered at 0.3– 1.5 kHz and was converted to digital pulses through a window discriminator (Neurolog; Digitimer). A computer using a custom-designed software written in LabVIEW (LabVIEW; National Instrument) was used to present the visual stimuli on a screen in front of the monkey, to deliver the reward and to store in real-time the force developed by the animal on the lever and the digital pulses from neuronal activity.

The microelectrode was lowered to isolate neurons while the monkey was performing the task. Single neurons were isolated from the background noise and from other neurons by continuously monitoring on an oscilloscope the waveform of the recorded neuronal impulses. Before recording in the STN, anterior limit of the external pallidal segment (GPe) was identified for another study (Nougaret and Ravel 2018) and neurons from both caudate nucleus and putamen were recorded (Nougaret and Ravel 2015). Additionally, the preliminary mapping we performed, based on the atlas of Saleem and Logothetis (2007), allowed us to map electrophysiologically the surrounding structure of the STN and was very helpful to define its boundaries. STN neurons were identified based on their firing characteristics described in previous studies (Wichmann et al., 1994; Darbaky et al., 2005; Isoda & Hikosaka, 2008; Espinosa-Parrilla et al., 2013, 2015) and on the characteristic firing patterns associated with neurons in regions dorsal and ventral to the structure that daily helped us to insure the localization of our recordings. Indeed, along the electrode trajectory, were encountered the thalamus, zona incerta, the STN and finally the substantia nigra pars reticulata (SNr) or pars compacta (SNc). The differences in the baseline activity of these structures and their background noises made clear the transitions between them. The very specific and high frequency activity of the SNr was particularly useful to confirm the localization of neurons previously recorded along the electrode track. The activity of the first well-isolated and stable STN unit in a trajectory was recorded for at least 10 trials per condition. After recording from a STN neuron, the electrode was moved forward until another STN neuron was encountered. Data from all STN neurons recorded were included in analyses.

Localization of Recordings

To assess the localization of our recordings, we used a high-resolution MRI scan for each monkey with electrodes positioned in trajectories from which we recorded neurons from the STN, the GPe and the striatum. MR images were collected using a T1-weighed sequence

(recovery time = 1700 msec, echo time = 4.414 msec, flip angle = 30°, in-plane resolution = 0.6 × 0.6 mm, thickness = 0.6 mm). On the basis of the localization of these electrode tips, we extrapolated the inferior/superior, anterior/posterior, and medial/lateral positions of each recorded neuron to generate a 3-D reconstruction of the whole neuronal population using Brainsight software (Brainsight; Rogue Research). The coordinates of each neurons were calculated based on their relative distance with the midpoint of the interaural line for each monkey. Because of the difficulties to clearly evidence the STN boundaries based on MR images, each neuron was then projected on a reconstruction of the STN based on the coordinates of its boundaries on the Atlas of Saleem and Logothetis (2007).

Data Analyses

All data analyses were performed using conventional statistical procedures with the R statistical computing environment (R Development Core Team, 2011), excepted the population decoding analysis that was performed using the neural decoding toolbox (Meyers 2013) on Matlab (The MathWorks, Inc., Natick, MA, USA). Data were analyzed from 8,469 trials performed (correct and incorrect) by the animals while a total of 78 STN neurons were recorded.

Behavioral Analyses

Two different measures were analyzed to evaluate the animal's behavior, the reaction times (RTs) and the acceptance levels. The RTs were defined as the duration between the onset of the cues and the time at which the monkey started to increase its pressing force on the lever and were only calculated for correct trials. After changed into z-scores for normalization purpose, a two-way ANOVA was performed with required force and expected reward as the two factors. Acceptance levels were computed by dividing the total number of trials accepted by the animal in a given condition (correct trials + holding and threshold errors) by the total number of trials proposed to the animal in this condition (trials accepted + omission errors) and compared with a Pearson's chi-squared test. This acceptance level reflects whether the animal chose to perform the task or not, depending on the level of force and the reward size. The force developed by the animals in each trial at each time of the task was collected and averaged by condition to highlight possible differences within a same range of force between two different reward conditions.

Electrophysiological Analysis

Response of STN neurons to the force and reward factors

We focused our analysis on the "cue-threshold period" (Figure 1A) that started with the occurrence of the cues and ended when the force developed on the lever exceeded the lower threshold of the force range. It corresponded to the period in which the animal saw the cues, integrated their significance and reacted to them accordingly to reach the required force range. The duration of this period varied across trials depending on the animal's behavior. In our task, the force required to correctly perform the trial, based on the shape of the stimuli and the force applied by the animals on the lever highly covariate and could not be inserted as factors of the same model for electrophysiological analysis. To disentangle the "motor" modulation, that is, modulation by the force applied by the animals on the lever, from the "factors" modulation, that is, the force required, the expected reward, and the interaction between both, we have performed a two-step iterative generalized linear model (GLM). First, we considered a model in which the force applied (*ForceApplied*) could be explained by the amount of required force (*Force*), the amount of expected reward (*Reward*), the interaction between both factors (*Force:Reward*) and a residual part not explained by these factors (*ResidualsForceApplied*) as follow:

$$ForceApplied = Force + Reward + Force{:}\,Reward + ResidualsForceApplied$$

The goal of this first iteration was to extract the residual part *ResidualsForceApplied*, that was the part of the force applied not explained by the factors. This part was then used in the second iteration together with the force and reward factors. It allowed to evaluate the modulation of the firing rate by the force applied, after the modulation by the factors had been extracted from it. We defined the second iteration as follow:

$$FiringRate = ResidualsForceApplied + Force + Reward + Force{:}\,Reward + ResidualsFiringRate$$

ResidualsForceApplied represented the modulation by the force applied on the lever not explained by the force and reward factors. *Force* represented the modulation by the amount of force required, *Reward* the modulation by the size of expected reward and *Force:Reward* the modulation by the interaction between both. *ResidualsFiringRate* represented the part of variance not explained by these variables. To minimize the probability of making Type I errors under the null hypothesis and to compensate the high risk of Family Wise Error rate due to multiple comparisons (78 neurons), we performed bootstrap analyses for the second iteration (Lindquist & Mejia, 2015; Maris & Oostenveld, 2007). This allowed us to compute *p values* without making assumptions on the distribution of the data. It consisted of randomly resampling the neuronal data to obtain replications of the same size as the original data set.

This procedure was performed 9999 times the analysis for each neuron, each time with a different resampling. The likelihood ratio was extracted for each resampled data set and compared with the one obtained from the original data set. Then, if the original likelihood ratio fell in the highest ventile (equivalent *p value* of .05), the neuron was considered to be significantly modulated by the factor of interest. The number of neurons modulated by the force applied and by the force and reward factors and their interaction were collected. For each neuron, a force selectivity index (FSI) and a reward selectivity index (RSI) were estimated. These selectivity indices (SI) were defined as follows:

$$SI = \frac{(\mu_1 - \mu_2)}{\sqrt{((SS_1 + SS_2)/(df_1 + df_2))}}$$

In this formula, μ_x was the mean of the *FiringRate* during the cue-threshold period. SS_x was the sum of the squares of the difference between the mean firing rate and the firing rate in an individual trial for each pair of condition described below. df_x was the degree of freedom (number of trials − 1) for each pair of conditions described below (Peck, Lau, & Salzman, 2013). For each neuron, the FSI was computed by comparing the neuronal activity during trials in the high force conditions (Fr and FR, represented by the subscript number 1) with the neuronal activity during trials in the low force conditions (fr and fR, represented by the subscript number 2). A positive FSI indicated a stronger modulation in the high force conditions, whereas a negative index indicated a stronger modulation in the low force conditions. In the same way, for each neuron, the RSI was computed comparing, the neuronal activity during trials in the large reward conditions (fR and FR, represented by the subscript number 1) with the neuronal activity during trials in the small reward conditions (fr and Fr, represented by the subscript number 2). A positive RSI indicated a stronger modulation in the large reward conditions, whereas a negative index indicated a stronger modulation in the small reward conditions.

Alignment on the Reaction time

The previous analysis was also performed in a 150-ms period following the RT to assess the influence of movement initiation on STN neuronal activity. As for the Cue-Threshold period, the number of significantly modulated neurons were computed and the selectivity indices were estimated during this period. The average spike-density was also calculated aligned on the reaction time to determine if the neural response was triggered by the cue onset or the movement initiation (Figure 3D). Because, it was clearly triggered by the cue onset, the analysis described later were only applied on the Cue-Threshold period and with the neuronal activity aligned on the cue onset.

Relation between the anatomical localization and the selectivity indices.

Each recorded neuron was reported on tridimensional representation of the brain and potential correlations between their localization inside the STN and their capacity to encode the factors of the task (FSI and RSI) were investigated. Pearson correlations were performed contrasting the FSI or the RSI of each neuron with its position in millimeters in antero-posteriority, laterality and depth.

Independence of subpopulations of neurons

The level of dependence between neurons belonging to subpopulations responding to the factors of the task was assessed using resampling methods. From the whole population of neurons (N), we defined the neurons selective for the amount of force N_{force}, the neurons selective for the amount of reward N_{reward} and the neurons selective for both, N_{FR}. Then, we reassigned randomly the previously computed *p values* for force and reward to have a simulated population of neurons. This resampling was performed 20,000 times and allowed us to have the distribution of the number of neurons N_{FR} found by chance. The position of our measured N_{FR} on this distribution allowed us to determine the dependency between both populations, i. e. if the encoding of a factor was predictive or preclusive to the encoding of the other factor.

Neural decoding analysis

We performed a neural decoding analysis using the neural decoding toolbox developed by Meyers (2013). This analysis used a maximum correlation coefficient classifier method trained to discriminate, in our case, among the 4 conditions of the task or between the two levels of a task factor, and to compute the decoding accuracy. Each recorded cell activity was formatted as a sequence of average activity by bins of 150 ms sampled at 20 ms intervals (overlap 130 ms) for each trial. For this population analysis, we first considered the whole population of 78 neurons and defined the optimal split factor (k = highest number of trials in each condition for each site). We decided to eliminate the 11 neurons with an insufficient number of trials in each condition for such analysis and to perform it on 67 neurons (sites) sharing at least 17 trials (k) per condition (4 x 17 = 68 data points). The following step was to randomly select from all the available data points of each site a population of 68 data points to shape a pseudopopulation of neurons (i. e. neurons recorded separately but treated as recorded simultaneously) with an equal number of data points.Then the data were normalized into z-score to allocate the same weight to each neuron and avoid the influence of a higher firing rate on the decoding method. The classifier was trained using k – 1 number of splits and next tested on the remaining split. This procedure was repeated 50 times to increase the strength of

the results, generating new splits and consequently new pseudopopulations. The results were then averaged over these 50 runs. To estimate the significativity of the classifier accuracy, a permutation test was performed by shuffling the labels and randomly assigned them to the conditions before re-running it. This procedure was repeated 10 times to obtain a null distribution of the decoding accuracies. The times when the decoding accuracies were above what was considered chance level were considered as statistically significant. The significance level was considered reached if the real decoding accuracies were greater than all the ones of the shuffle data in the null distribution for at least 5 consecutive significant bins. Always considering the whole population of neurons, when the decoding analysis of the force and reward factors was performed separately, we chose a k of 25 and 26 respectively, allowing us to consider 77/78 neuron and to remove only 1 cell. For the decoding analysis of the subpopulations of neurons modulated by the force or reward factors, we used different k, adapted for each situations. For the force modulated neurons (n = 19) we used, k = 13, 18 and 17 respectively to test the decoding of the condition, the reward factor and the force factor, allowing us to consider the whole population -1 (n=18) to test the condition, and the whole population (n = 19) to test the factors. For the reward modulated neurons (n = 15) we used, k =12, 26 and 25 to test the decoding for the condition, the reward factor and the force factor respectively. It allowed us to consider the whole population (n = 15) in all cases.

RESULTS

Behavioral results

Behavioral analyses were performed on trials completed while STN neurons were recorded (78 neurons, 30 from Monkey M, 16 days of recording and 48 from Monkey Y, 24 days of recordings).

Reaction Times

Average RTs (i.e. time to reach the lower threshold of the required force after the occurrence of cues) were computed from the correct trials only (2,337 from Monkey M and 3,942 from Monkey Y; Figure 2A). RTs were significantly shorter for the large reward trials than for the small reward ones in Monkey M (two-way ANOVA on RT z score, $p.reward < 0.001$, $F(1, 2333) = 95.9$) and in Monkey Y (two-way ANOVA on RT z score, $p.reward < 0.01$, $F(1, 3938) = 7.34$). Although there was a slight decrease in the high force condition for both monkeys, the two-way ANOVA revealed that there was no significant difference on the RTs between the high force trials and the low force trials (Monkey M, $p.force > 0.05$, $F(1,2333) =$

2.85; Monkey Y, p.force >0.05, F(1,3938) = 0.07). In both monkeys, there was no interaction effect between the required force level and the size of the expected reward on the RTs.

Acceptance level

Both monkeys shared an acceptance level, ordered from the highest to the lowest, for the conditions low force/high reward (fR), then high force/high reward (FR), then low force/small reward (fr), and finally high force/small reward (Fr) (Figure 2B). For both monkeys, the 4 conditions were thus ranked in the same preference order. The size of expected reward seemed to be more relevant than the level of effort required for them to decide whether to perform the task or not. In the most accepted fR conditions, monkeys decided to perform the action in 98.7% (Monkey M) and 98.9% (Monkey Y) of the trials. In contrast, in the least accepted Fr conditions, they only performed the action in 81.2% (Monkey M) and 87.7% (Monkey Y) of the trials. FR trials were accepted more frequently (96.9% for Monkey M and 96.3% for Monkey Y) than fr trials (86.0% for Monkey M and 94.2% for Monkey Y). The overall difference between the accepted trials and the rejected ones was highly significant for both monkeys (Monkey M: $\chi^2 = 191.05$, $p < 0.001$, Monkey Y: $\chi^2 = 157.03$, $p < 0.001$). Moreover, a 2-by-2 comparison revealed that each level of acceptance was different from the others (Monkey M: $\chi^2 > 4.93$, $p < 0.05$, Monkey Y: $\chi^2 = 5.67$, $p < 0.05$). These results show that the monkeys understood the task and have valued each condition before deciding to perform the trial or not. Indeed, the effort to be made and the size of the expected reward contributed to compute the subjective value of each condition for both monkeys. As depicted in Figure 2C, for the same amount of force required, the average force applied by the animals was slightly different depending on the expected/received reward in some periods. This result led us to consider the force applied as a variable in our analyses of the neuronal activity to isolate a reward or a force effect from motor response due to a mechanical modulation.

Electrophysiological Results

STN neurons activity during the cue-threshold period

Our visuomotor task allowed us to explore how STN neurons integrated visual cues carrying effort and reward-related information comparing to motor-related ones. During the cue-threshold period, corresponding to the period in which the visual stimuli significance was integrated and the response developed, 10.3% of neurons (8/78) modulated their activity depending on the force applied by the animal on the lever, while 36/78 (46.2%) modulated their activity depending on the task factors. Among these neurons, 19/36 (52.8%) showed a 'force effect', a difference in their activity between the high and low force trials, 15/36

(41.6%) showed a 'reward effect', a difference in their activity between large and small reward trials. It is important to note that only one cell belonged to both populations and that the group of neurons showing a force effect was independent of the one showing a reward effect (resampling method, equivalent p value = 0.065). The encoding of force was neither predictive nor preclusive to the encoding of reward and vice versa. On these 36 neurons, 4 showed an interaction effect (11,1%). The distribution of the force and reward selectivity indices for each of the 78 neurons and the average spike-density of the whole recorded population are shown in Figure 3. The overall distribution of the FSI during this period (Figure 3A, green histogram) was significantly positive and not centered on 0 (Wilcoxon signed rank test, V = 2279, p = 0.00023) and the RSI distribution showed the same tendency (Wilcoxon signed rank test, V = 1921, p-value = 0.0584, Figure 3A, red histogram). The window chosen for the analyis, between cue onset and threshold included the initiation of the movement by the animal. To control for the influence of movement initiation on the STN neuronal activity, the same analysis was performed but now aligned on the RT and the results compared with the one obtained for the Cue-Threshold period. During a period of 150 ms from the RT, 15.4% of neurons (12/78) modulated their activity depending on the force applied by the animal on the lever, while 26/78 (33.3%) modulated their activity depending on the task factors, 6 of them were present in both categories. The majority of them, 20/26 (76.9%), showed a 'reward effect', only 4/26 (15.4%) showed a force effect and 3/26 (11.5%) showed an interaction effect (Figure 3C). The overall distributions of FSI and RSI during this period showed the same but not significant tendency to be majoritarily positive than during the Cue-threshold period (Figure 3C, FSI: Wilcoxon signed rank test, V = 1860, p = 0.1115; RSI: Wilcoxon signed rank test, V = 1904, p = 0.07).

The average spike-density, aligned on cue onset or on RT (Figure 3D), shows that even if slighty higher when aligned on RT, the response of STN neurons was clearly triggered by the occurrence of the visual cues. For this reason, we considered the Cue-threshold period the most relevant to further analyze the activity of STN neurons, and this period will be the only one considered in the following analysis.

Distribution of the FSI and RSI of responding STN neurons

Among the 19 neurons showing a force effect, a significantly higher number of neurons (exact binomial test, p = 0.0007) were FSI+ (17/19; i.e. stronger response for the larger force) and the remaining ones FSI- (2/19; stronger response for the lower force). Conversely, among the 15 neurons showing a reward effect, a comparable number of neurons (exact binomial test, p = 0.61) were RSI+ (9/15) and RSI- (6/15). As illustrated in Figure 4A, the spike density

of the 19 neurons showing a force effect reflects the dominance of the FSI+ neurons and their response after the presentation of the cues. We did not observe any difference in terms of average spike density or distribution of the RSI for these 19 neurons, and the spike density of the conditions sharing the same force required (fr/fR and Fr/FR) was comparable. It was not the case for the 15 neurons showing a reward effect. Indeed, they were equally distributed between RSI+ and RSI- neurons (9 vs 6 neurons respectively). However, we observed a significant negative correlation between the force and reward indices of these 15 neurons (Pearson correlation, $r = -0.56$, $p = 0.028$) showing that the higher the RSI, the lower the FSI will be and the lower the RSI, the higher the FSI will be. This reveals that, even if not showing a force effect, most of the neurons showing a reward effect also integrate force value. Both subpopulations of reward modulated neurons (RSI+ and RSI-) were observed separately and revealed interesting features. The boxplot (Figure 4B, bottom left) and the average spike-density along time (Figure 4B, middle) show that the RSI+ and the RSI- neurons encoded the task conditions following the motivational ranking of the 4 task conditions (fR/FR/fr/Fr). Indeed, RSI + neurons increased their activity with the most favorable conditions of the task. At the single cell level, the raster shown on Figure 4B upper right evidenced this pattern of activity. As a population, we observed a tendency of positive correlation between their average activity in the cue-threshold period and the task conditions (Pearson correlation, $r = 0.23$, $p = 0.18$, Figure 4B, bottom left, “Positive RSI”). On the other hand, RSI- neurons decreased their activity in the most favorable conditions of the task. As a population, we observed a significant negative correlation between their average activity in the cue-threshold condition and the task conditions (Pearson correlation, $r = -0.44$, $p = 0.03$, Figure 4B, bottom left, “Negative RSI”). At the single celle level, the raster shown on Figure 4B bottom right evidenced this pattern of activity. As a whole, the reward modulated neurons encoded the motivational value conveyed by the visual stimuli rather than only the size of the reward by increasing or decreasing their activity according to the task conditions and their subjective value.

Neural decoding analysis

We performed a neural decoding analyis (Meyers, 2013) based on the training of a classifier to discriminate among the 4 different conditions, between both reward conditions (r and R) and between both force conditions (f and F). This analysis allowed us to evaluate three new aspects of the STN neuronal activity. The results are depicted in Figure 5. First, by performing the training of the classifier at one time point and testing its capacity to decode the activity at different time points (Figure 5A,B,C, left), we figured out whether the encoding of

the condition, force or reward information by STN neurons was static or dynamic. The dominance of the decoding accuracy confined along the main diagonal suggests that the representation of the condition and its factors was mainly sustained by a dynamic rather than a stationary code. The difference between these two representations is still a topic of interest but dynamic codes have been described to support complex stimulus transformation, as reported previously in studies interested in the representation of cognitive problems (Crowe et al. 2010), observed actions (Lanzilotto et al. 2019) and the ability to solve tasks more generally (Meyers 2018). The second and third aspects concern the temporal course of the decoding of information and the comparison of the decoding accuracy on selective and non-selective neurons. We observed, considering the whole neuronal population (Figure 5, middle) that the information regarding the amount of reward was integrated before (Figure 5B, middle, first significant bin: 160 ms after the occurrence of the cues, red curve) the information regarding the amount of force (Figure 5C, middle, first significant bin: 360 ms after the occurrence of the cues, green curve). Moreover, we evaluated the decoding accuracy of different neuronal populations, the neurons showing a reward effect, the neurons showing a force effect and the remaining neurons. Interestingly, the 15 neurons showing a reward effect (Figure 5A, right, red curve) decoded the task conditions 180 ms after the occurrence of the cues while the neurons showing a force effect significantly discriminate among the four conditions 700 ms after the occurrence of the cues. This main difference between both populations confirms our preceding analysis, the neurons showing a force effect were only involved in the encoding of the force whereas the neurons showing a reward effect also integrated a force information, allowing them to significantly decode among the task conditions. This result was confirmed when we looked further in the decoding of the force by the reward modulated neurons and vice versa. Indeed, even if late, the reward modulated neurons showed an increase in the decoding accuracy after the occurrence of the cues (Figure 5C, bottom, red curve) that the force modulated neurons did not show for the amount of reward at this time (Figure 6C, bottom, green curve).

Localization of the Recordings

The reconstruction of the electrode trajectories allowed us to extrapolate the location of each recorded neuron. The complete reconstruction along the 3 different planes is depicted on Figure 6. From the midpoint of the interaural line, the average coordinates of our recording were: laterality: 4.95mm ± 0.71 (min = 3.07mm, max = 6.68mm), antero-posteriority: 14.08mm ± 0.92 (min = 12.86mm, max = 16.01mm), depth = 11.29± 1.09 (min = 8.55, max = 13.75). Based of the reconstruction made from the atlas of Saleem and Logothetis (2007), the

majority of the recorded neurons were located in anterior half of the nucleus. We performed Pearson correlations to find potential link between the strength of STN neurons response (FSI or RSI) and the coordinates of the neuron's location (Laterality, Antero-posteriority and Depth). We found that, the neurons recorded more medially (Pearson correlation, $r = -0.24$, $p = 0.034$) and deeper (Pearson correlation , $r = 0.24$, $p = 0.031$) exhibited higher FSI. No significant correlation between the neuron's location and the RSI was found.

DISCUSSION

The present data brought new evidence about the functional properties of the STN neurons and their role in the integration of force, effort and motivational information. Our task allowed us to extract and differentiate information about 1) the encoding of force, i. e. the force developed physically on the lever, 2) the effort, i.e. the force requested on the lever in response to the green stimulus and 3) the motivation to act, i.e. an integration of the effort and the reward size to compute the motivational value specific of a pair of visual stimuli. First, we found that STN neurons, at single cell level, were mainly involved in independent processes with cells significantly modulated by the effort, i. e. the force requested to develop on the lever, or by the reward size, i. e. the amount of reward the animal can get at the end of the trial. Second, these two populations exhibited different patterns of modulation, the effort-modulated neurons were mainly active when a high effort was required, whereas the reward-modulated neurons did not only respond to the reward amount, but they also integrated, as a population, the motivational value of the stimuli. Third, the population of reward-modulated neurons was composed of neurons increasing or decreasing their activity in the most favorable condition of the task and exhibiting an activity according to the motivational ranking of the four task conditions. Fourth, the reward-modulated neurons seem to encode first the reward size and then integrate the amount of force required.

STN neurons encode the effort to produce rather than the force developed

Our results revealed an interesting feature about the STN neurons' properties. Indeed, during the cue-threshold period, when the animal must extract information from the cues and react to them accordingly, the proportion of neurons encoding the force required (low vs high) was higher than the proportion of neurons encoding the force developed. The work of Tan and colleagues (2013, 2015) showed similar evidence from recordings of the local field potentials (LFP) of STN of Parkinsonian patients (PD). They first showed a decreased power in the beta

band and an increased power in the gamma band when the effort required increased (Tan et al. 2013). In a second study (Tan et al. 2015), the authors disambiguate the effort from the force, asking the patients to exert different levels of force on a lever with the index or the little finger. For a same effort, a lower force was produced if the little finger was used. They demonstrated that STN activity encoded the effort rather than the absolute force and suggested a role of the basal ganglia in determining the effort to be attributed to a response more than in the parametrization of the movement itself. This is in line with behavioral studies in humans showing that individuals used the sense of effort more than the proprioceptive feedbacks to evaluate the force generation (Jones and Hunter, 1983, Carson et al. 2002, Proske et al. 2004). Recording the potentials evoked by transcranial magnetic stimulation of the motor cortex in peripheric muscles used in their task, Carson et al. (2002) showed that the sense of effort was not based on central motor command and proposed that is was associated with the activity of structures upstream of the motor cortex. The notion of effort to invest in an action was the center of the task performed by PD patients in the study of Zenon et al. (2016) that showed a neural response to the effort cues in the 1-10 Hz band of the STN LFP. Moreover, and in line with our results, the authors highlighted that the responses observed were more informative of the level of effort rather than the actual quantity of force. Interestingly, in our data, the deeper and the more medial the recordings, the higher the FSI. It has been recently demonstrated (Stephenson-Jones et al. 2016) that a pathway between the medial STN and the habenula-projecting globus pallidus (GPh) was involved in signaling when an outcome was aversive or worse than expected (Stephenson-Jones et al. 2019). We could hypothesize that the neurons encoding a high effort to be produced, located on the medial border of the STN, projected on the GPh and transferred a negative signal, to the lateral habenula. This hypothesis is supported by the fact that in rodents, a subpopulation of STN neurons could encode aversive reinforcers (Breysse et al. 2015). In a task similar to ours, Varazzani and colleagues (2015) reported a modulation of the noradrenergic neurons of the locus coeruleus (LC) by the task difficulty at the moment of the action. To date, no direct connections between the LC and the STN have been reported but we could hypothesize on an influence of LC effort-related activity on STN neurons indirectly through a prefrontal pathway. This last point is also supported by the fact that the force effect appeared later during the trial than the reward effect. It might well be possible that the reward-modulated neurons are directly sensitive to the cues information, while the force-modulated ones are reflecting a more integrated process like action preparation at some point.

STN neurons encode the motivational value of the combined visual stimuli

Neural correlates between STN neurons' activity and stimuli predictive of a reward or the reward itself have been previously shown in rodents (Baunez et al. 2002, 2005, Teagarden and Rebec 2007, Lardeux et al. 2009, 2013, Breysse et al. 2015, Baunez 2016) and in non-human primates (Matsumura et al. 1992, Darbaky et al. 2005, Espinosa-Parilla et al. 2013, 2015). The population of reward-modulated neurons we recorded also integrated, as a population, information about the force required, as shown by the negative correlation between the RSI and FSI of these neurons, and their ability to decode the condition and not only the reward size. STN neurons are known to be directly interconnected with a number of prefrontal areas (Takada et al. 2001, Nambu et al. 2002, Haynes and Haber, 2013) with some degree of overlap between STN territories (Haynes and Haber 2013, Nougaret et al. 2013). They would allow the gestion of conflict during decision-making by inhibiting the cortical activity through the STN-GPi-Thalamus-Cortex (GPi: Globus Pallidus internal segment) pathway. This enables a control of impulsivity by allocating a temporal window necessary for the scrutiny of the different available options (Frank et al. 2007, Cavanagh et al. 2011). The role of STN in the control of impulsivity and decision making has been largely documented in both rats and humans (see for review Eagle and Baunez, 2010; Breysse et al. 2020; Frank et al. 2007). In our study, this subpopulation of STN neurons could send a forerunner information to the output structures of the BG or to the GPe regarding the estimation of the subjective reward value, i.e. integrating also the effort in the valuation of the reward. This information would help at improving the decision-making, promoting or slowing down or stopping the execution of the action as suggested by Isoda and Hikosaka (2008). This computation could be under the influence of dopamine neurons known to play a role in value-based behaviors in a similar paradigm (Varazzani et al. 2015). Another target of these STN neurons could be the ventral pallidum (VP) with whom it shares reciprocal connections (Haber and Knuston 2010). The VP contains cells that display distinct reward modulations depending on the expected outcomes, the reward-positive and reward-negative types (Tachibana and Hikosaka 2012). Moreover, because the reward-positive neurons combined expected reward values and expected costs, the authors argued that the VP neuronal activity is used for modulating impending motor actions. Considering the reciprocal connections between the STN and the VP and the populations of positive and negative RSI neurons we found in the STN, we can hypothesize that these two structures would work together to update the value of a behavioral context and modulate a corresponding motor output. The temporal dynamic would be interesting to compare between the VP and STN. However, the present

study shows that the encoding of the reward size was a fast processing (180 ms) that occurs before integration with the force-related information. The fact that STN neurons are able to integrate both information in a sequential order is in line with the LFP recordings in PD patients tested in a similar task showing modulation of activity with regard to the net subjective value (Zenon et al 2016). Interestingly enough, these comparable results were obtained with a simultaneous combined cue presentation here, while in the task used with the patients, the cue indicating the size of the reward was presented before the cue related to the effort to produce (Zenon et al 2016). In monkeys, it has been reported (Espinosa-Parilla et al. 2015) that STN neurons are only sensitive to the value of the outcome at its occurence in the context of a choice. Here, we extend the precedent findings, showing the encoding of the motivational value of the visual stimuli by STN neurons, in the absence of choice to be made. The differences in the conclusions could be partly explained by the differences between the task used here and the one used by Espinosa-Parilla and colleagues, in the fact that, in our task, the reward amount varied but not its identity and, second, that various levels of force were needed and lead to different efforts, implying a cost-benefit integration.

Limitations of our interpretations and future perspectives

The present study demonstrates new features on STN neurons properties and completes our previous findings on the activity of the GPe neurons (Nougaret and Ravel 2018) and the tonically active neurons of the striatum (Nougaret and Ravel 2015) in the same paradigm. Indeed, the integration of the motivational value of the visual stimuli was only found in the STN as a population, placing this structure as an essential node modulating motivated behaviors within the BG circuitry. In our study, there was no choice to be made between two options, the choice was to perform or not the action and we recorded only few omission trials in each condition making difficult to study the monkey's decision to make the action or not, unlike in the study recording STN LFPs in Parkinsonian patients using a similar task (Zenon et al 2016). Consequently, our results raised conclusions about the incentive motivation rather than decision making about performing a motivated action. Moreover, to have a more complete view on how motivational information is processed within the BG, it would be of great interest to compare the properties of STN neurons with the ones of projection neurons of the striatum, the other main input structure of the circuit. Also, the STN is at the center of at least two main pathways within the basal ganglia, the indirect and the hyperdirect pathway, and our recordings did not allow us to identify whether the recorded neurons received mainly inputs directly from the cortex or indirectly through the striatum and the GPe. Complementary

studies involving inactivation of specific pathways could help to shed light on the contribution of each cortical and subcortical inputs in goal-directed behaviors and on STN neuronal responses. In addition, the understanding of how STN neurons encode motivational information appears fondamental to comprehend the non-motor neuropathologies involving dysfunctions of the BG such as addiction and obsessive compulsive disorders and the alterations of reward-based behaviors encountered in patients with Parkinson's Disease. Today, the deep brain stimulation of the STN (STN-DBS) introduced by Benabib and colleagues (Limousin et al. 1995) is used worldwide to alleviate the motor symptoms in PD patients but it also affects the cognitive and motivational deficits observed. Animal and clinical studies reported that STN-DBS can improve these non-motor deficits but can also make them worse (Chaudhuri and Shapira 2009; Castrioto et al. 2014), in some cases triggering an apathy that cancels the motor improvement observed in PD patients (Martinez-Fernandez et al . 2016). However STN-DBS can also reduce the oscillations between hypo and hyperdopaminergic states and diminish the compulsive use of dopaminergic medication and other forms of impulse control disorders observed in some PD patients (Lhommée et al. 2012; Eusebio et al. 2013). Interestingly, STN DBS applied in Parkinsonian patients performing a similar task to that used here increased their level of acceptance for trials involving a higher cost (Atkinson-Clément et al. 2019). This may be explained by either a faulty encoding of the effort or an increased motivation for the reward, in line with former studies showing an increased motivation for sweet food when an effort is required in a progressive ratio schedule of reinforcement (Rouaud et al. 2010), unlike when no effort is implied (Vachez et al. 2020). In contrast to what is reported with food reward, STN lesions or DBS reduce motivation for substances of abuse (cocaine, heroin and alcohol) (Baunez et al. 2005; Rouaud et al. 2010; Lardeux and Baunez 2008; Pelloux and Baunez 2017, Wade et al. 2017), suggesting it could be an interesting target for addiction treatment (Pelloux and Baunez 2013). Beneficial effects of STN DBS have been indeed shown on escalated heroin or cocaine intake (Wade et al. 2017; Pelloux et al. 2018). It was further shown that abnormal oscillatory activity within the STN might be associated with the escalated drug intake (Pelloux et al. 2018). Further work will thus be needed to understand more thoroughly how STN neuronal activity plays its role in motivational processes and how it could contribute to repair pathological states.

BIBLIOGRAPHY

709 Atkinson-Clement C, Cavazzini É, Zénon A, Witjas T, Fluchère F, Azulay JP, Baunez C,
710 Eusebio A. (2019) Effects of subthalamic nucleus stimulation and levodopa on decision-
711 making in Parkinson's disease. Mov Disord. 34(3):377-385.
712 https://doi.org/10.1002/mds.27625

713 Baunez C (2016) The Subthalamic Nucleus and Reward-Related Processes. J.-J.
714 Soghomonian (Ed.), Innovations in cognitive neuroscience. The basal ganglia: Novel
715 perspectives on motor and cognitive functions (p. 319–337). Springer International
716 Publishing. https://doi.org/10.1007/978-3-319-42743-0_14

717 Baunez C, Amalric M, Robbins TW (2002) Enhanced Food-Related Motivation after Bilateral
718 Lesions of the Subthalamic Nucleus. J Neurosci 22:562–568.

719 Baunez C, Dias C, Cador M, Amalric M (2005) The subthalamic nucleus exerts opposite
720 control on cocaine and "natural" rewards. Nat Neurosci 8:484–489.

721 Baunez C, Robbins TW (1997) Bilateral lesions of the subthalamic nucleus induce multiple
722 deficits in an attentional task in rats. Eur J Neurosci 9:2086–2099.
723 http://doi.wiley.com/10.1111/j.1460-9568.1997.tb01376.x

724 Breysse E, Meffre J, Pelloux Y, Winstanley CA, Baunez C. (2020) Decreased Risk-taking and
725 Loss chasing after Subthalamic Nucleus Lesion in Rats. Eur J Neurosci. 2020 Jul
726 6.https://doi.org/10.1111/ejn.14895

727 Breysse E, Pelloux Y, Baunez C (2015) The Good and Bad Differentially Encoded within the
728 Subthalamic Nucleus in Rats. eNeuro 2:e0014-15.

729 Brittain J, Watkins KE, Joundi RA, Ray NJ, Holland P, Green AL, Aziz TZ, Jenkinson N
730 (2012) A Role for the Subthalamic Nucleus in Response Inhibition during Conflict. J
731 Neurosci 32:13396–13401. https://doi.org/10.1523/JNEUROSCI.2259-12.2012

732 Carson RG, Riek S, Shahbazpour N (2002) Central and peripheral mediation of human force
733 sensation following eccentric or concentric contractions. J Physiol 539:913–925.
734 https://doi.org/10.1013/jphysiol.2001.013385

735 Castrioto A, Lhommée E, Moro E, Krack P (2014) Mood and behavioural effects of
736 subthalamic stimulation in Parkinson's disease. The Lancet Neurology 13:287–305.
737 https://doi.org/10.1016/S1474-4422(13)70294-1

738 Cavanagh JF, Wiecki T V, Cohen MX, Figueroa CM, Samanta J, Sherman SJ, Frank MJ
739 (2011) Subthalamic nucleus stimulation reverses mediofrontal influence over decision
740 threshold. Nat Neurosci 14:1462–1467. https://doi.org/10.1038/nn.2925

741 Chaudhuri KR, Schapira AH (2009) Non-motor symptoms of Parkinson's disease:
742 dopaminergic pathophysiology and treatment. The Lancet Neurology 8:464–474.
743 http://dx.doi.org/10.1016/S1474-4422(09)70068-7.

744 Coulthard EJ, Bogacz R, Javed S, Mooney LK, Murphy G, Keeley S, Whone AL (2012)
745 Distinct roles of dopamine and subthalamic nucleus in learning and probabilistic
746 decision making. Brain 135:3721–3734. https://doi.org/10.1093/brain/aws273

747 Crowe DA, Averbeck BB, Chafee M V (2010) Rapid Sequences of Population Activity
748 Patterns Dynamically Encode Task-Critical Spatial Information in Parietal Cortex. J
749 Neurophysiol 30:11640–11653. https://doi.org/10.1523/JNEUROSCI.0954-10.2010

750 Darbaky Y, Baunez C, Arecchi P, Legallet E, Apicella P (2005) Reward-related neuronal
751 activity in the subthalamic nucleus of the monkey. Neuroreport 16:1241–1244.
752 https://doi.org/10.1097/00001756-200508010-00022

753 Deffains M, Iskhakova L, Katabi S, Haber SN, Israel Z, Bergman H (2016) Subthalamic, not
754 striatal, activity correlates with basal ganglia downstream activity in normal and
755 parkinsonian monkeys. Elife 5:e16443. https://doi.org/10.7554/eLife.16443

756 Eagle DM, Baunez C. (2010) Is there an inhibitory-response-control system in the rat?
757 Evidence from anatomical and pharmacological studies of behavioral inhibition.
758 Neurosci Biobehav Rev.;34(1):50-72. https://doi.org/10.1016/j.neubiorev.2009.07.003

759 Espinosa-Parrilla JF, Baunez C, Apicella P (2015) Modulation of neuronal activity by reward
760 identity in the monkey subthalamic nucleus. Eur J Neurosci 42:1705–1717.
761 https://doi.org/10.1111/ejn.12938

762 Espinosa-Parrilla J-F, Baunez C, Apicella P (2013) Linking reward processing to behavioral
763 output: motor and motivational integration in the primate subthalamic nucleus. Front
764 Comput Neurosci 7:175. https://doi.org/10.3389/fncom.2013.00175

765 Eusebio A, Witjas T, Cohen J, Fluchère F, Jouve E, Régis J, Azulay JP (2013) Subthalamic
766 nucleus stimulation and compulsive use of dopaminergic medication in Parkinson's
767 disease. Journal of Neurology, Neurosurgery and Psychiatry 84:868–874.
768 https://doi.org/10.1136/jnnp-2012-302387

769 Frank MJ (2006) Hold your horses: a dynamic computational role for the subthalamic nucleus
770 in decision making. Neural Netw 19:1120–1136
771 https://doi.org/10.1016/j.neunet.2006.03.006

772 Frank MJ, Samanta J, Moustafa AA, Sherman SJ (2007) Hold Your Horses: Impulsivity,
773 Deep Brain Stimulation, and Medication in Parkinsonism. Science 318:1309–1312.

774 Fumagalli M, Rosa M, Giannicola G, Marceglia S, Lucchiari C, Servello D, Franzini A,
775 Pacchetti C, Romito L, Albanese A, Porta M, Pravettoni G, Priori A (2015) Subthalamic
776 involvement in monetary reward and its dysfunction in parkinsonian gamblers. J Neurol
777 Neurosurg Psychiatry 86:355–358. https://doi.org/10.1136/jnnp-2014-307912

778 Haber SN, Knutson B (2010) The Reward Circuit : Linking Primate Anatomy and Human
779 Imaging. Neuropsychopharmacology 35:4–26. http://dx.doi.org/10.1038/npp.2009.129

780 Haynes WIA, Haber SN (2013) The Organization of Prefrontal-Subthalamic Inputs in
781 Primates Provides an Anatomical Substrate for Both Functional Specificity and
782 Integration : Implications for Basal Ganglia Models and Deep Brain Stimulation. J
783 Neurosci 33:4804–4814. https://doi.org/10.1523/JNEUROSCI.4674-12.2013

784 Isoda M, Hikosaka O (2008) Role for subthalamic nucleus neurons in switching from
785 automatic to controlled eye movement. J Neurosci 28:7209–7218.

786 Jones LA, Depatiment P, Unit BE (1983) Effect of Fatigue on Force Sensation. Exp Neurol
787 81:640–650.

788 Lanzilotto M, Ferroni CG, Livi A, Gerbella M, Maranesi M, Borra E, Passarelli L, Gamberini
789 M, Fogassi L, Bonini L, Orban GA (2019) Anterior Intraparietal Area : A Hub in the
790 Observed Manipulative Action Network. Cereb Cortex 29:1816–1833.
791 https://doi.org/10.1093/cercor/bhz011

792 Lardeux S, Baunez C. (2008) Alcohol preference influences the subthalamic nucleus control
793 on motivation for alcohol in rats. Neuropsychopharmacology ;33(3):634-42.
794 https://doi.org/10.1038/sj.npp.1301432

795 Lardeux S, Paleressompoulle D, Pernaud R, Cador M, Baunez C (2013) Different populations
796 of subthalamic neurons encode cocaine vs . sucrose reward and predict future error. J
797 Neurophysiol 110:1497–1510.

798 Lardeux S, Pernaud R, Paleressompoulle D, Baunez C (2009) Beyond the Reward Pathway :
799 Coding Reward Magnitude and Error in the Rat Subthalamic Nucleus. J Neurophysiol
800 102:2526–2537. https://doi.org/10.1152/jn.91009.2008

801 Lhommée E et al. (2012) Subthalamic stimulation in Parkinson's disease: Restoring the
802 balance of motivated behaviours. Brain 135:1463–1477.
803 https://doi.org/10.1093/brain/aws078

804 Limousin P, Pollack P, Benazzouz A, Hoffman D, EBas J, Brouselle E, Perret J, AL. B (2005)
805 Effect on parkinsonian signs and subthalamic nucleus stimulation symptoms of bilateral.
806 Lancet 345:91–95.

807 Lindquist MA, Mejia A (2015) Zen and the art of multiple comparisons. Psychosom Med.
808 https://doi.org/10.1097/PSY.0000000000000148

809 Maris E, Oostenveld R (2007) Nonparametric statistical testing of EEG- and MEG-data. J
810 Neurosci Methods 164:177–190. https://doi.org/10.1016/j.jneumeth.2007.03.024

811 Martinez-Fernandez R, Pelissier P, Quesada JL, Klinger H, Lhommée E, Schmitt E, Fraix V,
812 Chabardes S, Mertens P, Castrioto A, Kistner A, Broussolle E, Pollak P, Thobois S,
813 Krack P (2016) Postoperative apathy can neutralise benefits in quality of life after
814 subthalamic stimulation for Parkinson's disease. Journal of Neurology, Neurosurgery
815 and Psychiatry 87:311–318. https://doi.org/10.1136/jnnp-2014-310189

816 Matsumura M, Kojima J, Gardiner TW, Hikosaka O (1992) Visual and Oculomotor Functions
817 of Monkey Subthalamic Nucleus. J Neurophysiol 67:1615–1632.

818 Merrill EG, Ainsworth A (1972) Glass-coated platinum-plated tungsten microelectrodes. Med
819 Biol Eng 10:662–672.

820 Meyers EM (2013) The neural decoding toolbox. Front Neuroinform 7:1–12.
821 https://doi.org/10.3389/fninf.2013.

822 Meyers EM (2018) Working Memory : Neural Mechanisms Dynamic population coding and
823 its relationship to working memory. J Neurophysiol:2260–2268.
824 https://doi.org/10.1152/jn.00225.2018

825 Mink JW (1996) The basal ganglia: focused selection and inhibition of competing motor
826 programs. Prog Neurobiol 50:381–425.

827 Nambu A, Tokuno H, Takada M (2002) Functional significance of the cortico-subthalamo-
828 pallidal 'hyperdirect' pathway. Neurosci Res 43:111–117.

829 Nougaret S, Meffre J, Duclos Y, Breysse E, Pelloux Y (2013) First evidence of a hyperdirect
830 prefrontal pathway in the primate : precise organization for new insights on subthalamic
831 nucleus functions. Front Comput Neurosci 7:1–2. https://doi.org/10.1038/19525

832 Nougaret S, Ravel S (2015) Modulation of tonically active neurons of the monkey striatum by
833 events carrying different force and reward information. Journal of Neuroscience
834 35:15214 –15226. https://doi.org/10.1523/JNEUROSCI.0039-15.2015

835 Nougaret S, Ravel S (2018) Dynamic Encoding of Effort and Reward throughout the
836 Execution of Action by External Globus Pallidus Neurons in Monkeys. J Cogn Neurosci
837 30:1130–1144. https://doi.org/10.1162/jocn

838 Peck CJ, Lau B, Salzman CD (2013) The primate amygdala combines information about
839 space and value. Nat Neurosci 16:340–348.

840 Pelloux Y, Baunez C (2013) Deep brain stimulation for addiction: Why the subthalamic
841 nucleus should be favored. Current Opinion in Neurobiology 23:713–720.
842 https://doi.org/10.1016/j.conb.2013.02.016

843 Pelloux Y, Baunez C (2017) Targeting the subthalamic nucleus in a preclinical model of
844 alcohol use disorder. Psychopharmacology (Berl) 234:2127-2137.
845 https://doi.org/10.1007/s00213-017-4618-5

846 Pelloux Y, Degoulet M, Tiran-Cappello A, Cohen C, Lardeux S, George O, Koob GF, Ahmed
847 SH, Baunez C. (2018) Subthalamic nucleus high frequency stimulation prevents and
848 reverses escalated cocaine use. Mol Psychiatry 23:2266-2276.
849 https://doi.org/10.1038/s41380-018-0080-y

850 Proske U, Weerakkody NS, Canny BJ (2004) Force matching errors following eccentric
851 exercise. Hum Mov Sci 23:365–378. https://doi.org/10.1016/j.humov.2004.08.012

852 R Development Core Team R (2011) R: A language and environment for statistical
853 computing Team RDC, ed. R Found Stat Comput 1:409 Available at: http://www.r-
854 project.org.

855 Rosa M, Fumagalli M, Giannicola G, Marceglia S, Lucchiari C, Servello D, Franzini A,
856 Pacchetti C, Romito L, Albanese A, Porta M, Pravettoni G, Priori A (2013) Pathological

857 Gambling in Parkinson ' s Disease : Subthalamic Oscillations During Economics
858 Decisions. Mov Disord 28:1644–1652. https://doi.org/10.1002/mds.25427

859 Rouaud T, Lardeux S, Panayotis N, Paleressompoulle D, Cador M, Baunez C (2010)
860 Reducing the desire for cocaine with subthalamic nucleus deep brain stimulation.
861 Proceedings of the National Academy of Sciences of the United States of America
862 107:1196–1200. https://doi.org/10.1073/pnas.0908189107

863 Saleem K, Logothetis N (2007) A combined MRI and histology atlas of the rhesus monkey
864 brain, San Diego: Academic Press.

865 Stephenson-Jones M (2019) Pallidal circuits for aversive motivation and learning. Curr Opin
866 Behav Sci 26:82–89. https://doi.org/10.1016/j.cobeha.2018.09.015

867 Stephenson-jones M, Yu K, Ahrens S, Tucciarone JM, Huijstee AN Van, Mejia LA, Penzo
868 MA, Tai L, Wilbrecht L, Li B (2016) A basal ganglia circuit for evaluating action
869 outcomes. Nature 539:289–293. https://doi.org/10.1038/nature19845

870 Tachibana Y, Hikosaka O (2012) Article The Primate Ventral Pallidum Encodes Expected
871 Reward Value and Regulates Motor Action. Neuron 76:826–837.
872 https://doi.org/10.1016/j.neuron.2012.09.030

873 Takada M, Tokuno H, Hamada I, Inase M, Ito Y, Imanishi M, Hasegawa N, Akazawa T,
874 Hatanaka N, Nambu A (2001) Organization of inputs from cingulate motor areas to basal
875 ganglia in macaque monkey. Eur J Neurosci 14:1633–1650.

876 Tan H, Pogosyan A, Anzak A, Ashkan K, Bogdanovic M, Green AL, Aziz T, Foltynie T,
877 Limousin P, Zrinzo L, Brown P (2013) Complementary roles of different oscillatory
878 activities in the subthalamic nucleus in coding motor effort in Parkinsonism. Exp Neurol
879 248:187–195. https://doi.org/10.1016/j.expneurol.2013.06.010

880 Tan H, Pogosyan XA, Ashkan K, Cheeran B, Fitzgerald JJ, Green AL, Aziz T, Foltynie T,
881 Limousin P, Zrinzo L, Brown P (2015) Subthalamic Nucleus Local Field Potential
882 Activity Helps Encode Motor Effort Rather Than Force in Parkinsonism. J Neurosci
883 35:5941–5949. https://doi.org/10.1523/JNEUROSCI.4609-14.2015

884 Teagarden MA, Rebec G V (2007) Subthalamic and Striatal Neurons Concurrently Process
885 Motor , Limbic , and Associative Information in Rats Performing an Operant Task. J
886 Neurophysiol 97:2042–2058. https://doi.org/10.1152/jn.00368.2006

887 Uslaner JM, Orco JMD, Pevzner A, Robinson TE (2008) The Influence of Subthalamic
888 Nucleus Lesions on Sign-Tracking to Stimuli Paired with Food and Drug Rewards :
889 Facilitation of Incentive Salience Attribution ? Neuropsychopharmacology:2352–2361.
890 https://doi.org/10.1038/sj.npp.1301653

891 Vachez Y, Carcenac C, Magnard R, Kerkerian-Le Goff L, Salin P, Savasta M, Carnicella S,
892 Boulet S (2020) Subthalamic Nucleus Stimulation Impairs Motivation: Implication for
893 Apathy in Parkinson's Disease. Movement Disorders 35:616–628.
894 https://doi.org/10.1002/mds.27953

895 Varazzani C, San-Galli A, Gilardeau S, Bouret S (2015). Noradrenaline and dopamine
896 neurons in the reward/effort trade-off: A direct electrophysiological comparison in
897 behaving monkeys. J Neurosci 35:7866–7877.
898 https://doi.org/10.1523/JNEUROSCI.0454-15.2015

899 Wade CL, Kallupi M, Hernandez DO, Breysse E, De Guglielmo G, Crawford E, Koob GF,
900 Schweitzer P, Baunez C, George O (2017). High-frequency stimulation of the
901 subthalamic nucleus blocks compulsive-like re-escalation of heroin taking in rats.
902 Neuropsychopharmacology 42:1850–1859. https://doi.org/10.1038/npp.2016.270

903 Wichmann T, Bergman H, Delong MR (1994) The Primate Subthalamic Nucleus . I .
904 Functional Properties in Intact Animals. J Neurophysiol 72:494–506.

905 Zavala BA, Tan H, Little S, Ashkan K, Hariz M, Foltynie T, Zrinzo L, Zaghloul KA, Brown
906 P (2014) Midline Frontal Cortex Low-Frequency Activity Drives Subthalamic Nucleus
907 Oscillations during Conflict. J Neurosci 34:7322–7333.
908 https://doi.org/10.1523/JNEUROSCI.1169-14.2014

909 Zénon A, Duclos Y, Carron R, Witjas T, Baunez C, Azulay J, Brown P, Eusebio A (2016)
910 The human subthalamic nucleus encodes the subjective value of reward and the cost of
911 effort during decision-making. Brain. 139:1830-1843.
912 https://doi.org/10.1093/brain/aww075

913

914 FIGURE LEGENDS

915

916 **Figure 1.** Task design and localization of the subthalamic nucleus recordings. A. Task design.
917 A trial started when the monkey applied a basal force on the lever and maintained it during a
918 one-second preparatory period after which a pair of visual stimuli appeared on the screen

(occurrence of the visual stimuli). In response to these stimuli, the monkey had to increase its pressing force until it reached the required force range materialized by a rectangle and a gauge on the screen (the time to reach the target force being the cue threshold period), and held its force for 1 second (i.e. holding period) to obtain the reward. B: Table illustrating the combinations of visual stimuli. Four possible pairs of visual stimuli indicated to the animal the force to be developed and the size of the upcoming reward. Green represented the force (F or f) and red the reward (R or r), a circle meant small (f or r) and a square meant large (F or R). The example condition shown in A was low force/large reward. C. Left. MR image from monkey Y (Left) and Monkey M (right) respectively at +13 mm and +14 mm from the midpoint of the interaural line. Both images have been reoriented to fit the electrode track (Monkey Y: angle AP -4.5/Lat 18; Monkey M: angle AP 6/Lat 17).

Figure 2. Behavioral performance of both monkeys. A. Reaction times (RT) of the monkeys in the 4 conditions of the task. r: small reward, R: large reward, solid black lines: high force, dashed black lines: low force. The error bars represent the standard error to the mean. The stars indicate the influence of force and reward on the animal reaction time (2-way ANOVA: **$p<0.01$, ***$p<0.001$). B. Acceptance level of the animals in the 4 conditions of the task (fR: low force/large reward; FR: high force/large reward; fr: low force/small reward; Fr: high force/small reward). The stars indicate significant difference between the proportions of accepted trials on the total number of trials performed in a given condition (Pearson's Chi-squared: *$p<0.05$, ***$p<0.001$). C. Mean of the force developed on the lever along the trial by the animals in the 4 conditions of the task. Black lines: high force, gray lines: low force, thick lines: large reward, thin lines: small reward. The dashed vertical line represents the occurrence of the visual stimuli.

Figure 3. Distribution of the FSI and RSI, average activity of STN neurons among the task conditions and comparison of cue versus RT alignement. A. Scatter plots of force- versus reward-selectivity indices for each individual neuron during the Cue-Threshold period. FSIs > 0 indicate higher modulation in the high force conditions. RSIs > 0 indicate higher modulation in the large reward conditions. The color of the dots indicates the significance of a modulation (force, reward or interaction effect) in the GLM analysis. Filled green circles represent the neurons showing a force effect. Unfilled red circles represent the neurons showing a reward effect. For scaling reason, a neuron with a RSI of 2.45 is not represented on the scatterplot. Black crosses represent neurons showing an interaction effect and small gray

dots represent neurons without modulation by the task factors. The superimposed histograms represent the distribution of the FSI (green) and the RSI (red) of the 78 neurons. B. Average spike-density (σ = 30) of the whole population (n = 78) of STN neurons. The horizontal dashed line represents the baseline activity and the 4 solid color lines the 4 conditions of the task (purple: fR, orange: FR, green: fr, blue: Fr). The vertical dashed line represents the occurrence of the visual cues. C. Same representation than in (A) for a period of 150 ms from the reaction time. D. Average spike-density (σ = 50) of the whole population all condition combined. The vertical dashed line represents the occurrence of the visual cues for the activity represented in blue and the RT for the acivity represented in gray. The activity is slighlty higher (<1Hz) when aligned on the RT but clearly triggered by the Cue onset.

Figure 4. Distributions of the FSIs and RSIs during the Cue-Threshold period and average spike-density of STN neurons showing a force or a reward effect. Same representation than in Figure 3. **A**. Indices distribution and average spike-density for the neurons showing a force effect. Left: Scatter plot of force- versus reward-selectivity indices for the neurons showing a force effect (n = 19; green filled circles). The black line represents the Pearson's correlation between the FSI and RSI of the 19 neurons. The gray arrow indicates the neuron taken as example on the right panel of the figure. Middle: the average spike-density shows the higher activity in the high force conditions after the occurrence of the cues (materialized by the vertical line at time 0). Right: raster plot of a cell showing a force effect. Each line represents a trial and each dot the occurrence of a spike. The trials are sorted among the 4 conditions. In this example, the activity is higher in the high force conditions than in the low force ones after the occurrence of the visual cues. **B**. Indices distribution and average spike-density for the neurons showing a reward effect. Left, up: Scatter plot of force- versus reward-selectivity indices for the neurons showing a reward effect (n = 15; empty red circles). The black line represents the Pearson's correlation between the RSI and FSI of the 15 neurons, revealing a significant correlation. The gray arrows indicate the neurons taken as example on the right panel of the figure. Middle: the average spike-density of the separated populations of neurons showing a reward effect. Middle, up: average spike-density of the neurons with a positive RSI (n = 9) showing higher activity in the large reward conditions after the occurrence of the cues (materialized by the vertical line at time 0), but also decreasing response with the high force. Middle, bottom: average spike-density of the neurons showing a negative RSI (n = 6) showing lower activity in the large reward conditions after the occurrence of the cues (materialized by the vertical line at time 0), but also increasing slightly with the high force.

Left, bottom: Boxplot representing the average activity during the Cue-threshold period and among the 4 conditions of the task of both subpopulations of reward modulated neurons RSI + and RSI -. The boxplots illustrate the influence of the force on the reward modulated neurons. Only for RSI -, the effect of force is significant. Purple: fR; orange: fR; green: fr; blue: Fr. Right: Raster plots of neurons showing a positive (up) and a negative (bottom) reward effect at the occurrence of the cues. The influence of the force on the reward modulated neurons is visible at the population and at the single cell-level.

Figure 5. Dynamic encoding of relevant information of the task along the trial. **A**. Results obtained following the training of a classifier at a time t_1 (y-axis) and testing this classifier at a time t_2 (x-axis) for the decoding of the task condition. Left: Bi-dimensional map of the decoding accuracy in which each pixel represents the decoding accuracy at a time t_2 with a training of the classifier performed at t_1. The higher decoding accuracy along the main diagonal shows the dynamic decoding of the task condition. The black lines indicate the occurrence of the visual cues. Middle: the black curve represents the decoding accuracy along the main diagonal, at lag 0 (when $t_1 = t_2$) for the whole population of recorded neurons. Right : Similar representation analyzing separately the neurons showing a force effect (green), a reward effect (red) and the remaining ones (gray). The thick lines at the bottom of the plots represent the significance of the decoding accuracy above the chance level (at 25%, 4 conditions). The time is the beginning of the first of five significant consecutive bins based on the same analysis performed with a shuffle of the condition labels. **B. and C**. Same representation than in A. for the decoding of the amount of reward (**B**) and the amount of force (**C**). The trials are pooled between the small reward (fr and Fr) conditions versus the large reward (fR and FR) conditions for the decoding of the amount of reward. Inversely, they are pooled between the low force (fr and fR) conditions versus the high force conditions (Fr and FR) for the decoding of the amount of force. The chance level represented by the black line is 50% in both cases.

Figure 6. Topography of the neuronal recordings in the subthalamic nucleus. The three bidimensional plots on the left represent the projections of each recorded cell from the midpoint of the interaural line. Up left: AP vs Laterality: horizontal view. Up right: Depth vs Laterality: coronal view. Bottom left: Depth vs AP, sagittal view. Right: three-dimensional reconstruction of the cell distribution and theoretical boundaries of the STN based on the atlas of Saleem and Logothetis (2007). The filled circles represent the neurons recorded in Monkey

1021 Y and the filled squares the neurons recorded in Monkey M. The ellipsoids on the
1022 bidimensional plots represent the 95% of the cell distribution for each population of cells,
1023 green: neurons showing a force effect (n = 19), red: neurons showing a reward effect (n = 15),
1024 black: remaining neurons (n= 45).
1025

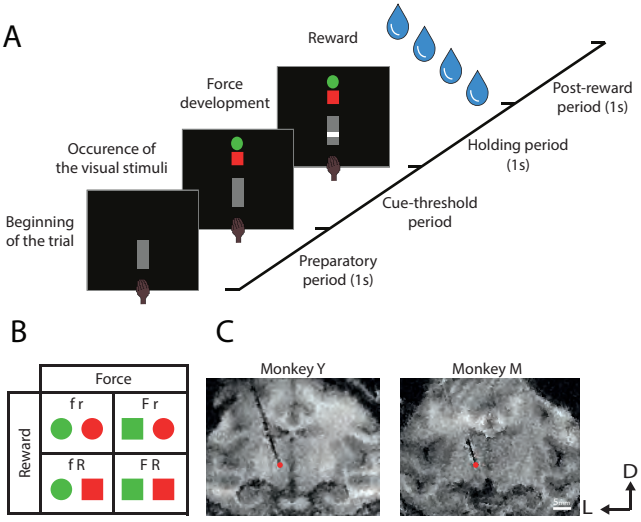

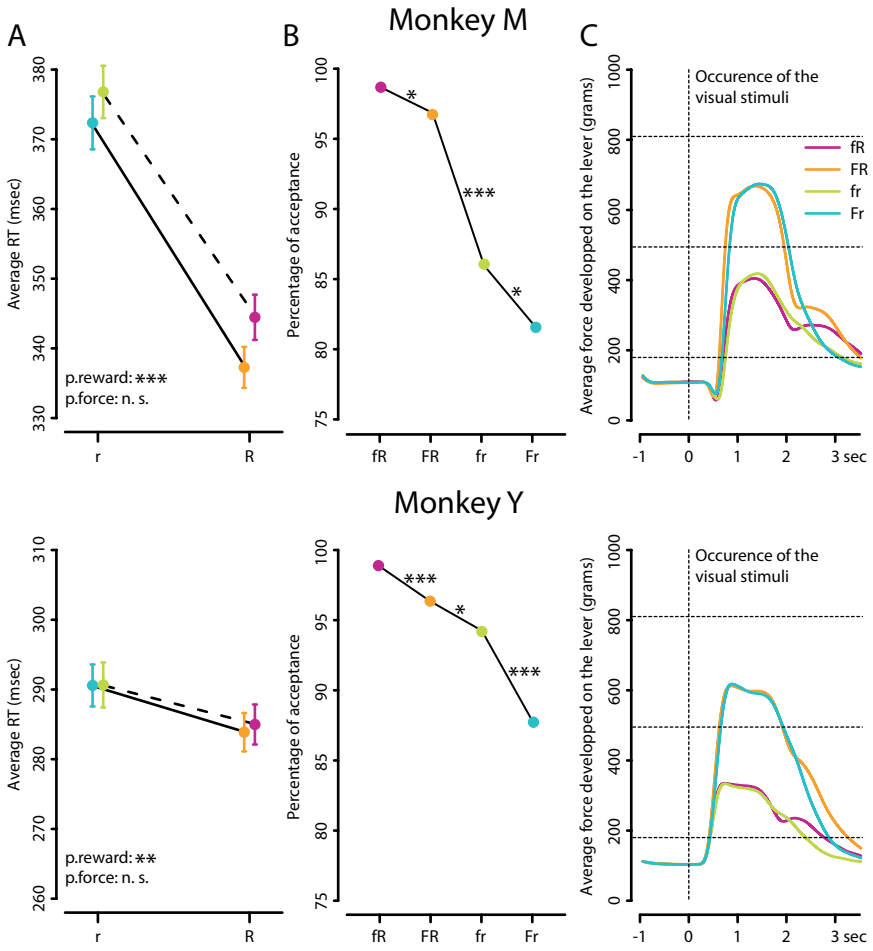

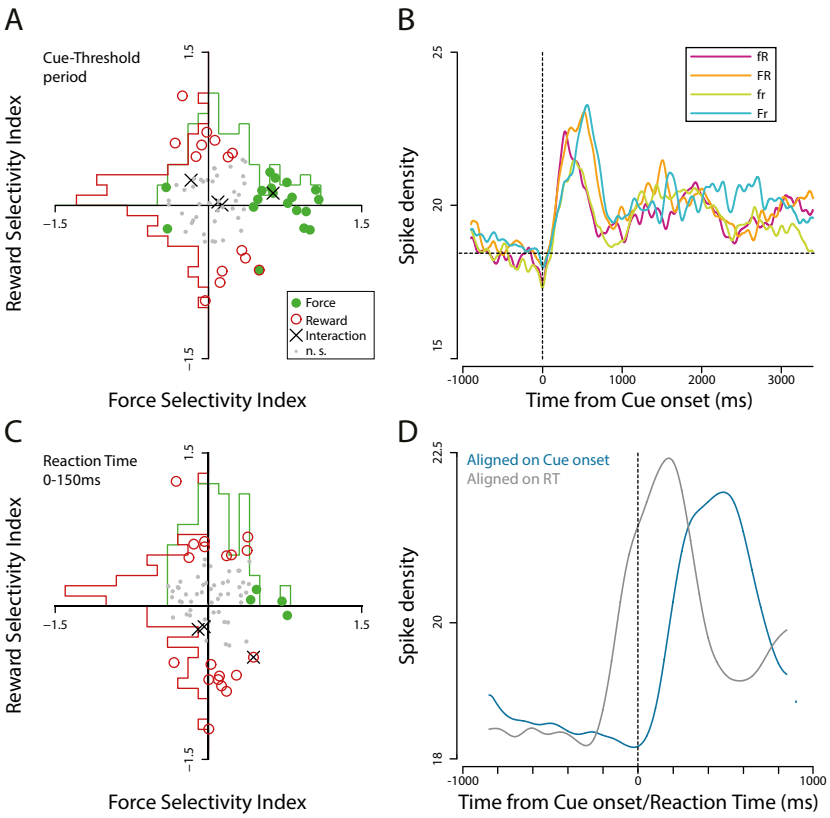

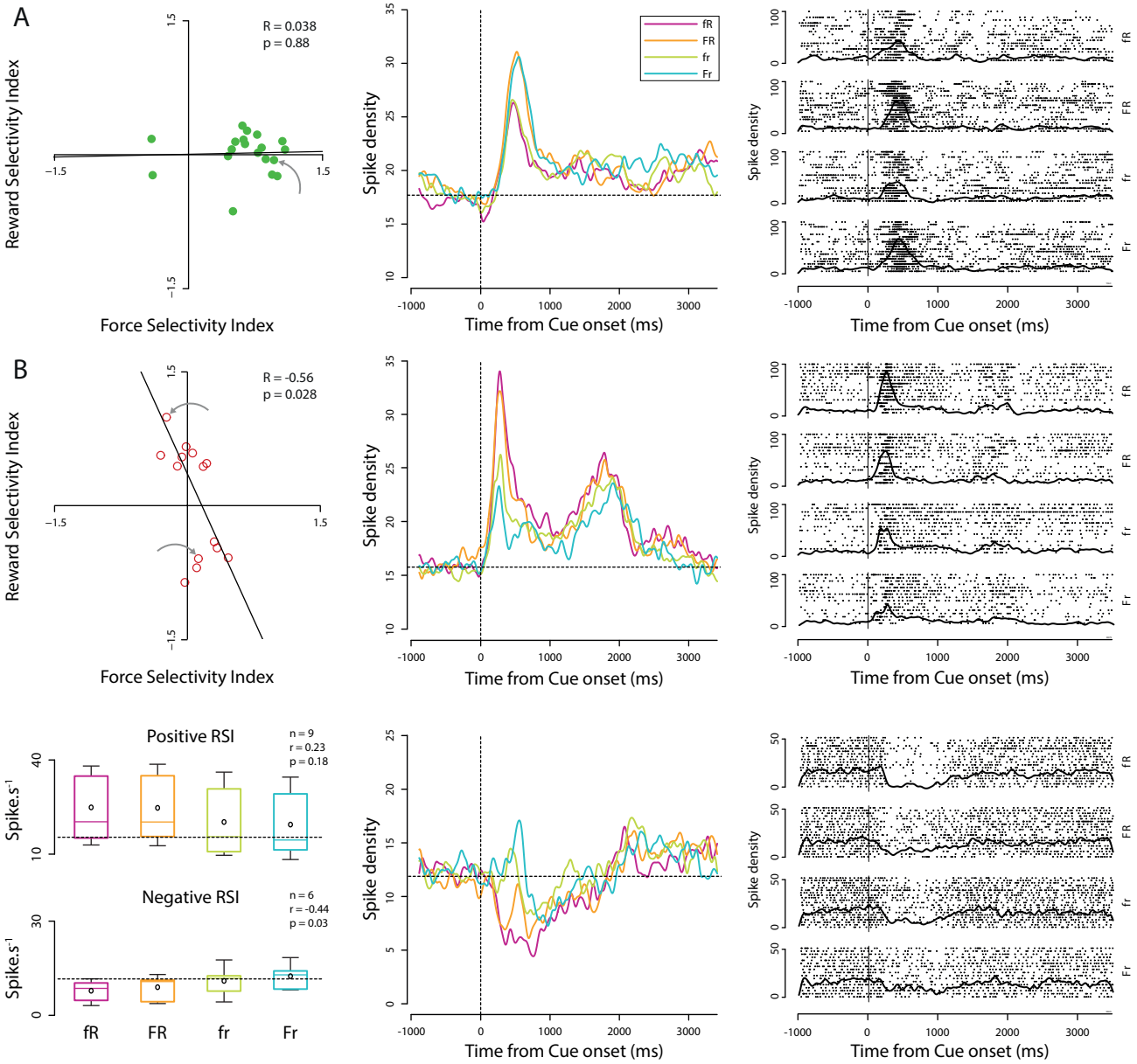

A

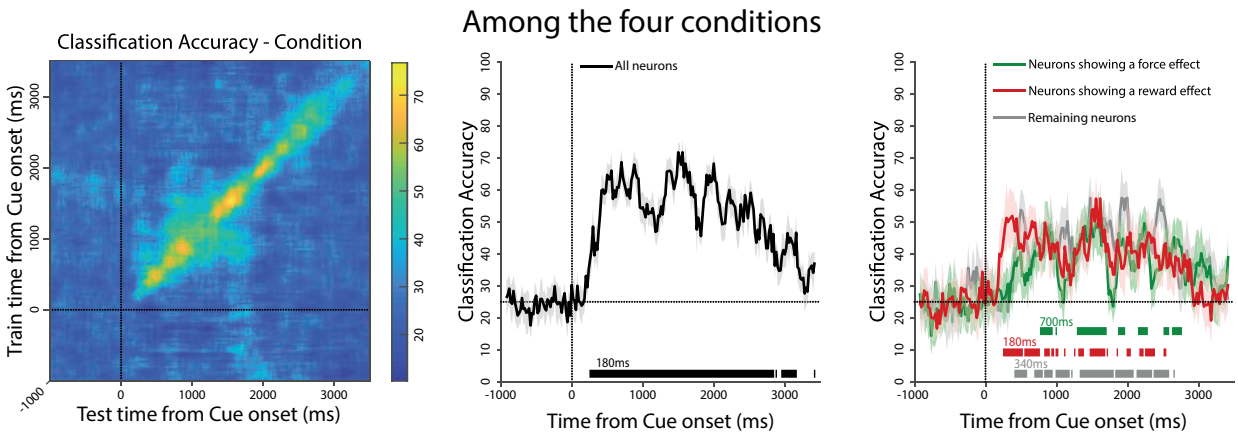

B

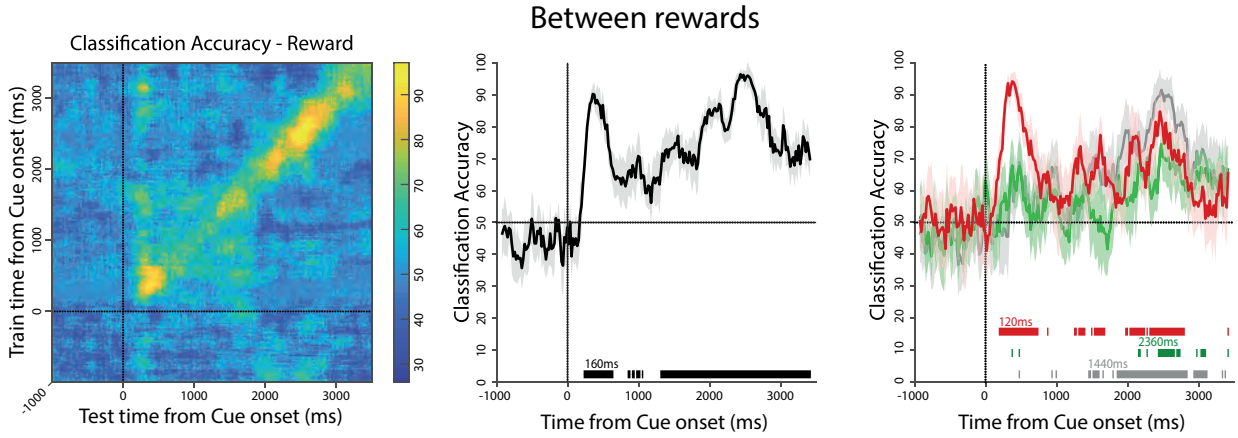

C